Waveguide branches in photonic crystals

Shanhui Fan, S. G. Johnson, and J. D. Joannopoulos

*Department of Physics, Massachusetts Institute of Technology, 77 Massachusetts Avenue,
Cambridge, Massachusetts 02139*

C. Manolatou and H. A. Haus

*Department of Electrical Engineering and Computer Science, Massachusetts Institute of Technology,
77 Massachusetts Avenue, Cambridge, Massachusetts 02139*

Theoretical and numerical analyses of waveguide branches in a photonic crystal are presented. Conditions for perfect transmission and zero reflection are discussed. Based upon these conditions, numerical simulations of electromagnetic-wave propagation in photonic crystals are performed to identify structures with near-complete transmission. © 2001 Optical Society of America

OCIS codes: 130.1750, 130.2790, 230.7370, 230.1360.

1. INTRODUCTION

Waveguide branches play an important role in integrated photonic circuits. Ideally, such a device splits the input power into the two output waveguides without significant reflection or radiation losses. Motivated by the goal of miniaturizing photonic components and circuits, there have been many efforts to construct wide-angle branches.[1–5] Despite such efforts, the splitting angles are still limited to a few degrees for conventional structures, owing to the inherent radiation loss at the branching region. Moreover, while such loss can be substantially reduced,[6,7] it cannot be completely suppressed by increasing the index contrast between the guide and the surrounding media. Photonic crystals offer the way to completely eliminate radiation losses[8] and thereby open the possibility of designing wide-angle branches with high performance. Very recently, estimates of the transmission characteristics of a 120° Y branch in a crystal with hexagonal symmetry have been presented by Yonekura *et al.*[9] However, direct and accurate numerical characterizations of the transmission and reflection properties through a single waveguide branch have not been previously performed. Moreover, a general criterion for ideal performance of waveguide branches in a photonic crystal has yet to be developed. In this paper we present theoretical calculations for the construction of a waveguide branch in a photonic crystal. We note that structures with 120° rotational symmetry, including the configuration considered by Yonekura *et al.*,[9] do not completely eliminate reflection. Based upon our theoretical considerations, we introduce designs of photonic-crystal waveguide branches with 180° branching angles that display near-zero reflection and almost-complete transmission.

2. THEORETICAL CONSIDERATIONS

In order to obtain a qualitative understanding of waveguide branches in a photonic crystal, we consider the theoretical model,[7] as shown in Fig. 1. The branching region is treated as a cavity that couples to the input and output waveguides. The resonance in the cavity then determines the transport properties of the branch.

The transmission and reflection properties of such a model can be calculated by use of coupled-mode theory,[10] which relates the incoming and outgoing wave amplitudes S_{+i} and S_{-i} at port i, to the amplitude of the resonant mode a, as follows:

$$\frac{da}{dt} = j\omega_0 a - a\left(\sum_i \frac{1}{\tau_i}\right) + \sum_i \left(S_{+i}\sqrt{\frac{2}{\tau_i}}\right), \quad (1)$$

$$S_{-i} = -S_{+i} + \sqrt{\frac{2}{\tau_i}}a. \quad (2)$$

Here, ω_0 is the resonant frequency, and $1/\tau_i$ is the amplitude decay rate of the resonance into the ith port. Also, for simplicity we have assumed a single-mode cavity. When the electromagnetic wave at a frequency ω is incident upon the system from port 1, i.e., $S_{+2} = S_{+3} = 0$, the reflection coefficient R and the transmission coefficients T_2 and T_3 into the remaining two ports can be determined as

$$R = \left|\frac{S_{-1}}{S_{+1}}\right|^2 = \left|\frac{-j(\omega - \omega_0) + \dfrac{1}{\tau_1} - \dfrac{1}{\tau_2} - \dfrac{1}{\tau_3}}{j(\omega - \omega_0) + \dfrac{1}{\tau_1} + \dfrac{1}{\tau_2} + \dfrac{1}{\tau_3}}\right|^2, \quad (3)$$

$$T_2 = \left|\frac{S_{+2}}{S_{+1}}\right|^2 = \left|\frac{\dfrac{2}{\sqrt{\tau_1 \tau_2}}}{j(\omega - \omega_0) + \dfrac{1}{\tau_1} + \dfrac{1}{\tau_2} + \dfrac{1}{\tau_3}}\right|^2,$$

$$(4)$$

$$T_3 = \left| \frac{S_{+3}}{S_{+1}} \right|^2 = \left| \frac{\frac{2}{\sqrt{\tau_1 \tau_3}}}{j(\omega - \omega_0) + \frac{1}{\tau_1} + \frac{1}{\tau_2} + \frac{1}{\tau_3}} \right|^2 . \tag{5}$$

From Eq. (3), zero reflection can be achieved at the resonant frequency $\omega = \omega_0$, if the rate-matching condition

$$\frac{1}{\tau_1} = \frac{1}{\tau_2} + \frac{1}{\tau_3} \tag{6}$$

is satisfied. Furthermore, the power is split evenly between port 2 and port 3 in a symmetric situation when $1/\tau_2 = 1/\tau_3$.

In Fig. 2 we plot the transmission coefficient T_2 at the resonant frequency as a function of the decay rates, assuming the symmetric situation where $1/\tau_2 = 1/\tau_3$. Ideal splitting, i.e., a 50% transmission coefficient, occurs at the optimal ratio $\tau_1/\tau_2 = 0.5$. We also note that the transmission coefficient is only a slowly varying function of the ratio τ_1/τ_2. Transmission higher than 45%, for example, can be achieved with τ_1/τ_2 ranging from 0.26 to 0.97. Therefore, while ideal performance can only be
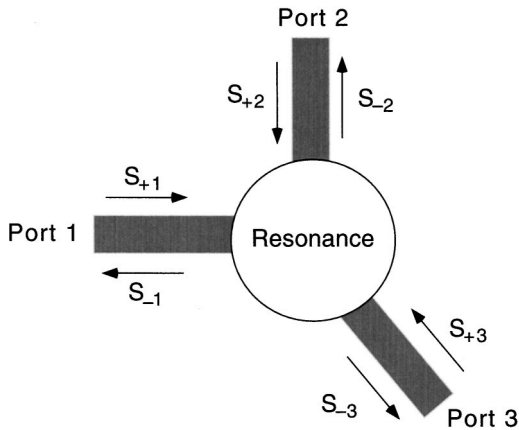

Fig. 1. Schematic of the theoretical model for waveguide branches. The gray regions represent the waveguides, and the white circle represents a resonator. S_{+i} and S_{-i} are the input and output wave amplitudes at the ith port, respectively.
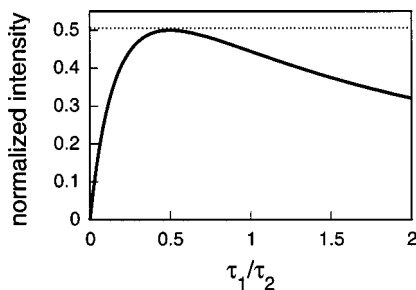

Fig. 2. Prediction of the theoretical model as shown in Fig. 1, assuming that the wave is incident from port 1 and that the output ports are symmetric. Plotted here is the intensity-transmission coefficient into port 2, as a function of the ratio between the decay rates into the input and an output waveguide.

achieved with an exact matching of the decay rates, one expects many structures to have relatively high transmission.

In particular we first consider structures with C_{3v} symmetry (i.e., the symmetry group of an equilateral triangle). In the case where the resonance is singly degenerate, the decay rates into the three ports are equal, i.e., $\tau_1 = \tau_2 = \tau_3$, which leads to a transmission coefficient of 4/9 at resonance. Whereas the coupled-mode analysis is approximate, this case in fact provides the exact upper limit of transmission for any structure with 120° rotational symmetry.

To see that, we note that in general, the incoming amplitudes $\mathbf{S}_+ = (S_{+1},..., S_{+n})$ are related to the outgoing amplitudes $\mathbf{S}_- = (S_{-1},..., S_{-n})$ by a scattering matrix T, i.e.,

$$\mathbf{S}_- = T \cdot \mathbf{S}_+ . \tag{7}$$

Energy conservation and time-reversal symmetry require that the matrix T be symmetric and unitary.[10] For structures with C_{3v} symmetry the matrix T therefore assumes the following form:

$$T = \begin{bmatrix} \alpha & \beta & \beta \\ \beta & \alpha & \beta \\ \beta & \beta & \alpha \end{bmatrix}, \tag{8}$$

where $|\alpha|^2$ and $|\beta|^2$ are the reflection and transmission coefficients. In addition, since T is unitary, α and β must satisfy the following conditions:

$$|\alpha|^2 + 2|\beta|^2 = 1, \tag{9}$$

$$|\beta|^2 + \alpha\beta^* + \alpha^*\beta = 0. \tag{10}$$

Defining $\varphi = \arg(\alpha\beta^*)$, we immediately obtain

$$|\alpha|^2 = \frac{1}{1 + 8 \cos^2 \varphi} \geq \frac{1}{9}, \tag{11}$$

which puts a lower limit on the reflection coefficient. Thus we have shown that for structures with threefold rotational symmetry the maximum transmitted intensity into either of the output ports cannot exceed 4/9 of the incoming intensity. This result, in fact, is well known in microwave circuit design.[11]

3.   NUMERICAL SIMULATIONS

Based upon the theoretical calculations presented above, we choose to study structures without threefold rotational symmetry. We perform numerical simulations of T-shaped waveguide branches in a two-dimensional photonic crystal made of a square lattice of dielectric rods in air ($\epsilon=1$), which has a gap in the TM modes.[8] The computational cell is shown in Fig. 3. The rods have a dielectric constant ϵ of 11.56 and a radius of $0.2a$, where a is the lattice constant. The waveguides are introduced by removing rows or columns of rods in the crystal.[8]

We simulate the propagation of electromagnetic waves using finite-difference time-domain methods[12] with perfectly-matched-layer boundary conditions.[13] Fifteen grid points are used to represent each lattice constant. A dipole source located at the entrance of the input wave-
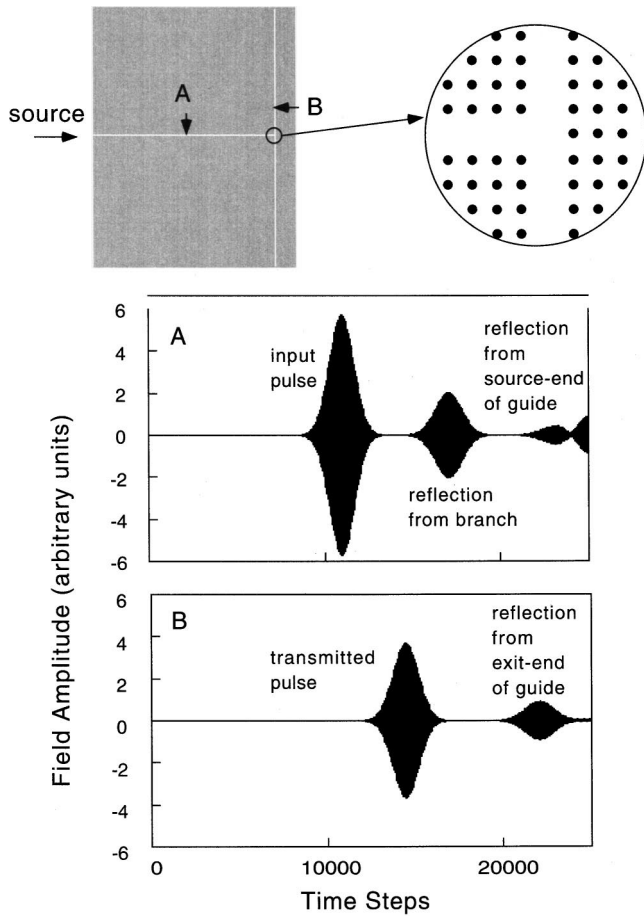
Fig. 3.   Top panel: Schematic view of the $140a \times 180a$ computational cell, where a is the lattice constant.   The field amplitude is monitored at points A and B, which are placed in the input and output guides of the branch, respectively.   The output guide is separated from the edge of the cell by ten periods of rods.   Bottom panel: Field amplitude recorded at points A and B, as a function of time.   The pulses reflected by and transmitted through the branch, as well as the pulses reflected from the edges of the cell, are easily discernible.
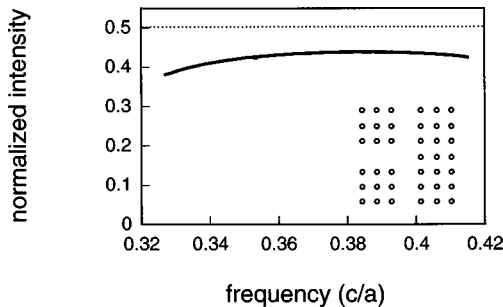

Fig. 4.   Intensity-transmission spectra through the waveguide branch shown in Fig. 3.   The structure of the branching region is also shown in the inset.

guide creates a pulse with a Gaussian envelope in time. The field amplitude is monitored before the branch (point A) and after the branch (point B), as indicated in the top panel of Fig. 3.   Although most of the light that reaches the edge of the crystal escapes and is absorbed by the boundaries, some light gets reflected back from the ends of the waveguides.   By using a sizable computational cell

of 140×180 lattice constants and by positioning each monitor point appropriately, we can distinguish and separate all the different pulses propagating in the cell: the useful pulses, such as the input pulse and the pulse reflected by and transmitted through the branch, and the parasite pulses, which are reflected from the edges of the crystal.   These pulses are clearly shown in the bottom panel of Fig. 3.   In the simulations, four pulses are sent down the guide, each covering different ranges of frequencies.   The pulses are then Fourier transformed to obtain the reflection and transmission coefficients for each frequency.   The reflection coefficients and the combined transmission coefficients into the two output arms add up to unity to within an accuracy of 0.1%, indicating that our approach indeed eliminates the error associated with the reflection from the edge of the crystal and gives an accurate description to the response function of the waveguide branch.

For the T-shaped structure shown in Fig. 3 the transmission spectra thus obtained are shown in Fig. 4.   The transmission coefficient is a slow varying function of the frequency: it remains higher than 42% for a wide range of frequencies between $0.348(2\pi c/a)$ and $0.415(2\pi c/a)$, with a maximum of 43.8% at the frequency $\omega = 0.387(2\pi c/a)$.

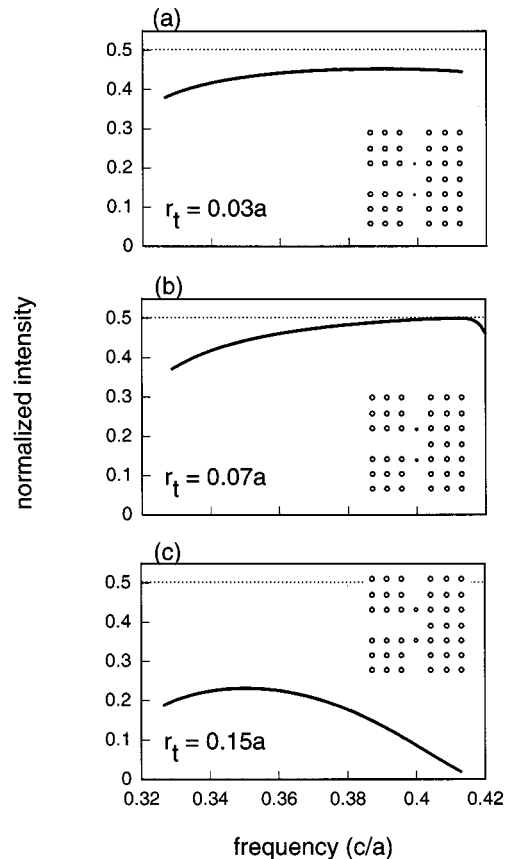We can qualitatively explain the simulation results using the coupled-mode theory arguments presented above.

Fig. 5.   Intensity-transmission spectra for waveguide-branch structures with (a) $r_t = 0.03a$, (b) $r_t = 0.07a$, and (c) $r_t = 0.15a$.   The structures are shown in the inset of each panel. The r_t denotes the radius of the smaller rods between the input and output waveguides.
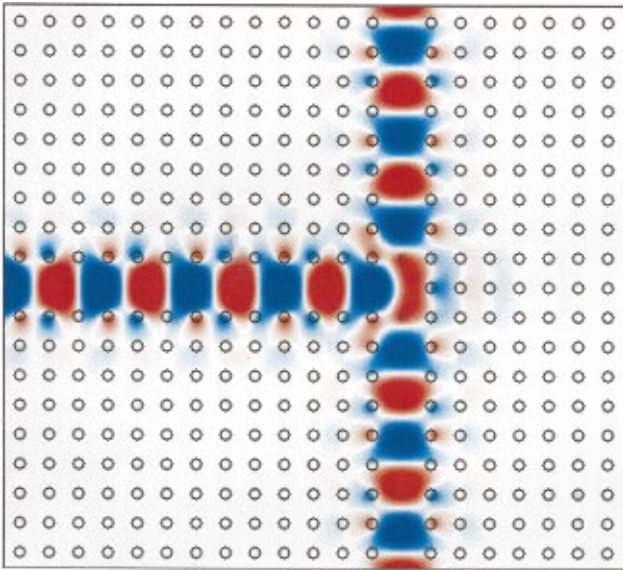
Fig. 6. Steady-state electric field distribution, at a frequency $\omega = 0.41(2\pi c/a)$, for the waveguide-branch structures with $r_t = 0.07a$, as shown in Fig. 5(b). Red and blue represent large positive and negative fields, while white represents zero field.

We approximate the cavity region by a point defect formed by removing one rod from the perfect crystal. Such a defect creates a localized state that possesses the full symmetry of the lattice.[8] The localized state therefore should couple to all the input and output waveguides with substantially the same strength, resulting in a peak transmission of 44.4%, in qualitative agreement with the simulation.

In order to improve the transmission we therefore need to reduce slightly the coupling between the resonance and the output waveguides, to satisfy the rate-matching condition described by Eq. (6). This is achieved by placing extra rods between the input and output waveguides (Fig. 5). The radius r_t of these extra rods is then varied for performance optimization. As r_t is increased from zero, the transmission is significantly improved, as shown in Figs. 5(a) and 5(b). In the case where $r_t = 0.07a$ [Fig. 5(b)] the transmission coefficient remains higher than 49.5% within the frequency range between $\omega = 0.398(2\pi c/a)$ and $\omega = 0.416(2\pi c/a)$ [Fig. 5(b)]. [The drop in transmission at frequencies above $0.417(2\pi c/a)$ is due primarily to an increase in tunneling of light from the output arms to the outside of the crystal because of the increased coupling to bulk states at the upper band edge.] Further increasing r_t to $0.15a$, however, results in a deviation from the rate-matching condition [Eq. (6)] and therefore leads to a decrease in transmission, as shown in Fig. 5(c).

In Fig. 6 we plot the steady-state field distribution at $\omega = 0.41(2\pi c/a)$ for the structure with $r_t = 0.07a$. The fields are completely confined within the waveguide regions and split equally into the output waveguides.

4. SUMMARY

We have presented a theoretical analysis of waveguide branches in photonic crystals. We have identified optimized structures by simulating the propagation of electromagnetic waves in a two-dimensional photonic crystal.

ACKNOWLEDGMENT

REFERENCES

1. M. Rangaraj, M. Minakata, and S. Kawakami, "Low loss integrated optical Y-branch," J. Lightwave Technol. **7**, 753–758 (1989).
2. H. Hatami-Hanza, M. J. Lederer, P. L. Chu, and I. M. Skinner, "A novel wide-angle low-loss dielectric slab waveguide Y-branch," J. Lightwave Technol. **12**, 208–214 (1994).
3. A. Klekaump, P. Kersten, and W. Rehm, "An improved single-mode Y-branch design for cascaded 1:2 splitters," J. Lightwave Technol. **14**, 2684–2686 (1996).
4. M. H. Hu, J. Z. Huang, R. Scanrmozzino, M. Levy, and R. M. Osgood, "A low-loss and compact waveguide Y-branch using refractive-index tapering," IEEE Photonic Technol. Lett. **9**, 203–205 (1997).
5. H.-B. Lin, J.-Y. Su, R.-S. Cheng, and W.-S. Wang, "Novel optical single-mode asymmetric Y-branches for variable power splitting," IEEE J. Quantum Electron. **35**, 1092–1096 (1999).
6. J. S. Foresi, D. R. Lim, L. Liao, A. M. Agarwal, and L. C. Kimerling, "Small radius bends and large angle splitters in SOI waveguides," Proc. SPIE **3007**, 112–118 (1997).
7. C. Manolatou, S. G. Johnson, S. Fan, P. R. Villeneuve, H. A. Haus, and J. D. Joannopoulos, "High-density integrated optics," J. Lightwave Technol. **17**, 1682–1692 (1999).
8. J. D. Joannopoulos, P. R. Villeneuve, and S. Fan, "Photonic crystals: putting a new twist on light," Nature **386**, 143–149 (1997).
9. J. Yonekura, M. Ikeda, and T. Baba, "Analysis of finite 2-D photonic crystals and lightwave devices using the scattering matrix method," J. Lightwave Technol. **17**, 1500–1508 (1999).
10. H. A. Haus, *Waves and Fields in Optoelectronics* (Prentice-Hall, Englewood Cliffs, N.J., 1984).
11. K. Kurokawa, *An Introduction to the Theory of Microwave Circuits* (Academic, New York, 1969).
12. For a review, see K. S. Kunz and R. J. Luebbers, *The Finite Difference Time Domain Method for Electromagnetics* (CRC Press, Boca Raton, Fla., 1993); and A. Taflove, *Computational Electrodynamics: The Finite-Difference Time-Domain Method* (Artech House, Norwood, Mass., 1995).
13. J. C. Chen and K. Li, "Quartic perfectly matched layers for dielectric waveguides and gratings," Microwave Opt. Technol. Lett. **10**, 319–323 (1995).